Eur. Phys. J. A **11**, 147–154 (2001)

THE EUROPEAN PHYSICAL JOURNAL A

Phase shift analysis and extraction of structure functions for Coulomb distortion on (e, e′p) reactions at high electron energies

K.S. Kim[1,a], Myung Ki Cheoun[2], Yeungun Chung[3], and Hyung Joo Nam[4]

[1] BK21 Physics Research Division and Institute of Basic Science, Sung Kyun Kwan, University, Suwon, 440-746, Korea
[2] Accelerator Mass Spectrometry Laboratory, Seoul National University, Seoul, 151-742, Korea
[3] Department of Physics, Yosu National University, Yosu, 550-250, Korea
[4] Department of Physics, Chung-Ang University, Seoul 156-756, Korea

Received: 4 January 2001 / Revised version: 5 April 2001
Communicated by M. Garçon

Abstract. In this paper we improve our approximate phase shifts of the electron wave functions by including Coulomb distortion effects from medium and heavy nuclei on exclusive $(e, e'p)$ reactions in the quasielastic region. The new phase shifts are parameterized for the elastic electron scattering and work very well at incident electron energies greater than 300 MeV. The structure functions with the new phase shifts for the electron wave functions are extracted. We use a relativistic single-particle model as applied to ^{208}Pb and to recently measured data at CEBAF on ^{16}O$(e, e'p)$ to investigate the electron Coulomb distortion effects and to extract the structure functions with the new phase shifts.

PACS. 25.30.Fj Inelastic electron scattering to continuum – 25.70.Bc Elastic and quasielastic scattering

1 Introduction

Electron scattering has long been acknowledged as one of the most excellent tools for investigating nuclear structure and nuclear properties, especially in the quasielastic region. One of the primary treatments is the plane-wave Born approximation (PWBA) in which the electron Coulomb distortion is neglected. The cross-section in the PWBA can be written as a sum of bilinear products of electron kinematics and nuclear structure functions as a function of energy and momentum transfer. Various structure functions for the process can be extracted from the measured data by the so-called Rosenbluth separation methods. In principle, the structure functions are independently calculated in the PWBA calculations, since they appear in the cross-section with different electron kinematics factors.

The inclusion of the electron Coulomb distortion in elastic and inelastic scattering has been done to various approximations in the past [1–5]. The Coulomb distortion has been exactly treated by fully expanding partial waves [6–9] of the electron wave functions, according to a method called distorted-wave Born approximation (DWBA), obtained by numerically solving the radial Dirac equation for a finite nuclear charge distribution. Although the electron Coulomb distortion can be treated exactly, this calculation presents numerical difficulties and the computational time increases rapidly with higher incident electron energy. Furthermore, it is no longer possible to separate the cross-section into the various structure functions with the partial-wave expansion in the presence of the electron Coulomb distortion. Nevertheless, in the early 1990s, the Ohio University group [6–11] treated the electron Coulomb distortion for the exclusive $(e, e'p)$ and the inclusive (e, e') reactions in the quasielasatic region very well.

Another approach to the inclusion of the Coulomb distortion for a large momentum transfer was developed by Knoll [12] in the early seventies. Lenz and Rosenfelder [13] then constructed an approximate high-energy wave functions given in analytic form by replacing the exact electron wave functions. This approximation to the wave functions, called the effective momentum approximation (EMA), was shown to be good to first order in αZ for high-energy scattering at short range, as shown by Giusti and Pacati. They expanded the exponential phase shift operator [14]. However, it turned out that the expansion does not converge very well [15] and the approximation is not good enough for heavy nuclei. Traini and Covi, with a realistic nuclear model, obtained good agreement with experimental data by using the EMA calculation [16].

To avoid these difficulties, recently the Ohio group [17–19] developed an approximate treatment of the Coulomb distorted electron wave functions, which contains an r-dependence instead of the static Coulomb potential which

[a] e-mail: kyungsik@earth.phys.cau.ac.kr

is evaluated at the origin in the effective momentum, hence called the local effective momentum approximation (LEMA). These wave functions have a "plane-wave–like" form that *directly allows* the extraction of the various structure functions from the cross-section as in the PWBA calculation. The Ohio group compared their approximate treatment of Coulomb distortion to the full DWBA results and found a good agreement of about 1-2% near the peaks of the cross-section even for a heavy nucleus like ^{208}Pb. In carrying out these calculations the range of the incident electron energies was restricted to 300-500 MeV. Recently, a new experiment was performed with incident electron energies higher than 2000 MeV at CEBAF [20]. In this energy range, it is very difficult to include the Coulomb distortion because many partial waves are needed. But Kim and Wright [21] introduced an improved "plane-wave–like" form for the wave functions, called the approximate DWBA, by parameterizing the phase shifts. Their results describe the experimental data from CEBAF very well.

The Ohio group calculation of the (e, e') reactions used the same potential for both bound and continuum states to avoid the violation of orthogonality, current conservation, and gauge invariance [7]. In the calculation (single-particle model), the knocked-out nucleon does not necessarily leave the nucleus without further interaction. However, since the subsequent interactions do not affect the (e, e') cross-sections, the potential used does not contain an absorptive part. The free Dirac current operator was used in the calculations, and the bound and continuum wave functions were solutions to the Dirac equation with the scalar and the vector potential calculated in the relativistic Hartree model. The results of this model are shown to be relatively high in comparison to the data on the longitudinal response function. For the transverse response functions the calculations at backward angle were smaller than the data. The calculations were carried out in the quasielastic region and the meson exchange current as well as the Δ excitation were not taken into account. From these comparisons, it appears that the meson exchange current and the Δ excitation need to be taken into account on the transverse response functions at backward angle (or large energy transfer). The approach of the Ohio group is less time consuming in comparison with a full DWBA procedure, but has some *ad hoc* assumptions: they choose the momentum transfer $\mathbf{q}(\mathbf{r})$ instead of the asymptotic momentum transfer $\mathbf{q}$ along the $\hat{\mathbf{z}}$-axis, so that they use the local electron kinematics $\left(\frac{q(r)_\mu^2}{q(r)^2}\right)^2$, etc., as factorizing the Rosenbluth terms inside the integrations in order to avoid destroying the separable form. They also use an *ad hoc* term to avoid the numerical difficulty involved in the electron phases. For the case of positron scattering, their calculation shows a discrepancy with new experimental data measured at Saclay [22]. Recently, the Ohio group calculated the positron scattering with the inclusion of the average of the electron phases [23], but they still found disagreement with the experimental data.

On the other hand, the structure functions cannot be directly extracted from the measured cross-section, but it is possible to extract a couple of functions, the fourth and the fifth structure functions which embody the left-right and up-down asymmetries of the cross-section, measured with respect to the missing momentum, by using the PWBA formalism. The structure functions for the $(e, e'p)$ reactions are affected by the final-state interaction of the knocked-out proton. Once the initial nucleon wave function is known, the structure functions provide information on the final-state interaction and on the nuclear structure, that is, the propagation of the knocked-out proton in the nucleus. Thus, each structure function might be useful to discriminate among theoretical models. Especially, the fifth structure function is known to vanish in the absence of the final-state interactions of the knocked-out proton [24]. In this case, the extraction of the fifth structure function requires a polarized incident electron beam.

In sect. 2 of this paper, we briefly review the previous approximation of the Coulomb distorted electron wave functions and present a greatly improved parameterization of the phase shifts. We apply the new phase shifts to heavy nuclei like ^{208}Pb. In sect. 3, we introduce a formalism for the $(e, e'p)$ reactions and a method to extract the second, fourth, and fifth structure functions and the asymmetry using the approximate DWBA calculation. A relativistic Hartree single-particle model (σ-ω model) for the bound state [25] and a relativistic optical model for the outgoing proton [26] are used. We calculate the extracted structure functions and asymmetry from the $p_{1/2}$ and $p_{3/2}$ orbits of the ^{16}O$(e, e'p)$ reaction and compare them with the new experimental data measured at CEBAF [20] in sect. 4. Conclusions are given in sect. 5.

2 Phase analysis

In an approximate way, Kim and Wright [18] constructed the following "plane-wave–like" electron wave functions which contain the effect of the static Coulomb distortion of the target nucleus:

$$\Psi^{\pm}(\mathbf{r}) = \frac{p'(r)}{p}\; e^{\pm i\delta(\mathbf{L}^2)}\; e^{i\Delta}\; e^{i\mathbf{p}'(r)\cdot\mathbf{r}}\; u_p\;, \qquad (1)$$

where the phase factor $\delta(\mathbf{L}^2)$ is a function of the square of the angular momentum operator, u_p denotes the Dirac spinor, and the local effective momentum $\mathbf{p}'(r)$ is given in terms of the Coulomb potential of the target nucleus by

$$\mathbf{p}'(r) = \left(p - \frac{1}{r}\int_0^r V(r)\mathrm{d}r \right) \hat{\mathbf{p}}\;. \qquad (2)$$

We referred to this r-dependent momentum as the LEMA. The *ad hoc* term $\Delta = a[\hat{\mathbf{p}}'(r)\cdot\mathbf{r}](\mathbf{J}^2 + \frac{1}{4})$ denotes a small higher-order correction which involves $a = -\alpha Z(16/p)^2$. The number 16 is given in MeV/c and was determined by comparison with the exact partial-wave result. Since the eigenvalues of $\mathbf{J}^2 = (\mathbf{L} + \mathbf{S})^2$ are $j(j+1)$ which is equal to $\kappa^2 - \frac{1}{4}$, the phase factor could be expanded up to the

second-order term and fitted to the exact phases with the equation

$$\delta_\kappa = b_0 + b_2\kappa^2 + b_4\kappa^4 \,, \tag{3}$$

where the coefficients, b_0, b_2, b_4 are fitted values. κ is a Dirac quantum number. We referred to these phases as the κ^2-dependent phases. The phases work very well for κ values up to approximately $\kappa = 3pR \approx 35$ at medium or low energy, but break down for $\kappa = 3pR \geq 50$. p denotes the electron momentum and the nuclear radius R is given by $R = 1.2A^{1/3} - 0.86/A^{1/3}$.

In order to solve this problem, we build new approximate phase shifts which can be applied to any incident energies and any κ values. The phases due to the Coulomb distortion of the target nucleus approach the point Coulomb phases for very high κ values (long distance from the target). It is difficult to fit the part around the surface of the target nucleus. We use the exact phase values at $\kappa = 1$ and at $\kappa = pR$ and then, we solve the equation of the approximate phases. Hence, we obtain the new phase shifts for a large incident electron energy as

$$\delta(\kappa) = \left[a_0 + a_2\frac{\kappa^2}{(pR)^2}\right]e^{-\frac{1.4\kappa^2}{(pR)^2}} - \frac{\alpha Z}{2}(1 - e^{-\frac{\kappa^2}{(pR)^2}})\times\ln(1+\kappa^2)\,. \tag{4}$$

We fit the two constants a_0 and a_2 to two of the elastic scattering phase shifts ($\kappa = 1$ and $\kappa = \mathrm{Int}(pR) + 5$). To have a very good approximation, we put $a_0 = \delta(1)$ and $a_2 = 4\delta(\mathrm{Int}(pR)+5) + \alpha Z\ln(2pR)$. As shown in fig. 1, the κ^2-dependent phases break down for high κ values, but the new phases reproduce the exact phases very well for ^{16}O with an electron energy $E = 2400$ MeV. However, the new phases have a small discrepancy in comparison with the exact phase around $\kappa = 30$, *i.e.*, around the surface of the target nucleus. Since we choose the maximum κ value to be $\kappa_{\max} = 3pR \approx 100$, $\kappa = 30$ is around the surface of the target nucleus. We refer to this new phase shift plus the LEMA as the approximate DWBA.

With the approximate DWBA discussed in the above paragraph, we construct the new "plane-wave–like" wave functions for the incoming and outgoing electrons. Since the only spinor dependence is in the Dirac spinor, all the Dirac algebra goes through in the common manner. The four-potential for the electron current becomes a Möller-type potential which contains an r-dependent momentum transfer $q(r)$. Using "plane-wave–like" electron wave functions, the corresponding cross-section can be separated into nuclear structure functions as in the PWBA formalism. Consequently, the structure functions can be directly calculated even in the presence of the electron Coulomb distortion. A detailed discussion can be found in refs. [17, 18]. In the present work we compare the directly calculated structure functions with the structure functions extracted in sect. 3.

As a test case, we calculate the reduced cross-section of the $(e, e'p)$ reactions with the new phases for a heavy

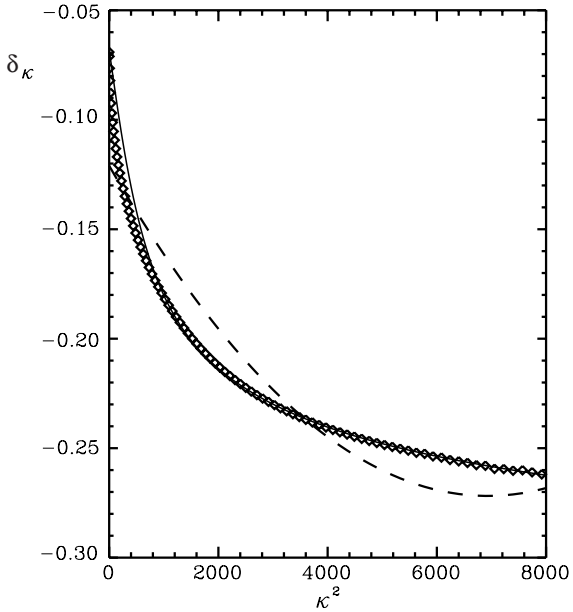

Fig. 1. Comparison between the exact, κ^2-dependent, and the new phases in ^{16}O for $\kappa_{\max} = 100$ and energy $E = 2441$ MeV. The diamonds are the exact phases, the dashed curve is the κ^2 fit, and the solid curve the new phase shifts parameterization.

nucleus. If the electron and the outgoing proton are described as plane waves, the reduced cross-section

$$\rho_m(p_m) = \frac{1}{pE\sigma_{ep}}\frac{\mathrm{d}^3\sigma}{\mathrm{d}E_f\mathrm{d}\Omega_f\mathrm{d}\Omega_p}\,, \tag{5}$$

is the probability that the proton, bound in a given shell, is met inside the nucleus with missing momentum $\mathbf{p}_m = \mathbf{p} - \mathbf{q}$. The off-shell electron-proton cross-section σ_{ep} denotes the form "cc1" given by de Forest [27]. Figure 2 shows the reduced cross-sections as a function of the missing momentum p_m for the $3s_{1/2}$ energy shell of ^{208}Pb. The kinematics are the incident electron energy $E_i = 412$ MeV, and the outgoing proton kinetic energy $T_p = 100$ MeV. The solid line is the result of the full DWBA [7], the dashed curve is the result with the new phase shifts, and the dotted curve is the result with the κ^2-dependent phases. The dashed curve obtained with the new phases describes the full DWBA result better than the κ^2-dependent phases result over the whole region.

3 Extraction of structure functions

We choose the nucleus in a fixed frame where it is placed at the origin of the coordinate system in the laboratory reference frame. As shown in fig. 3, the incoming electron with four-momentum $p_i^\mu = (E_i,\ \mathbf{p}_i)$ and the outgoing electron with $p_f^\mu = (E_f,\ \mathbf{p}_f)$ define the scattering plane (x-z plane). The knocked-out proton with $p^\mu = (E, \mathbf{p})$ and four-momentum transfer $q^\mu = p_i^\mu - p_f^\mu$ define the reaction plane. We choose the $\hat{\mathbf{z}}$-axis along the momentum transfer $\mathbf{q}$ direction. In the PWBA, the cross-section for the

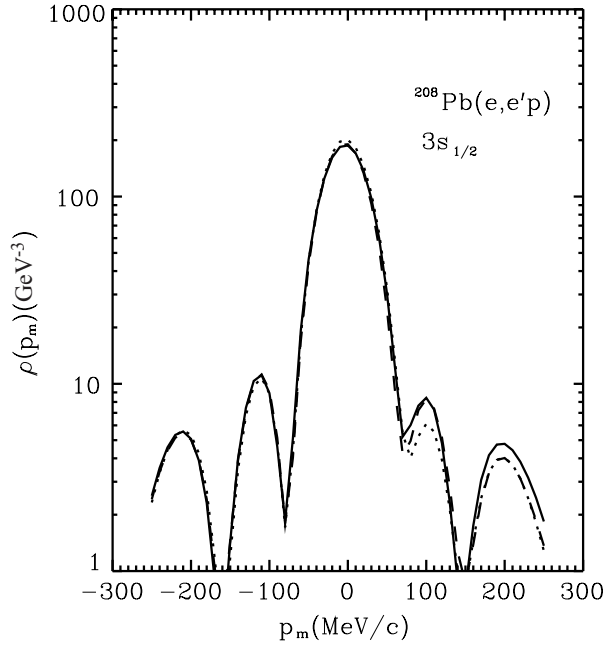

Fig. 2. The reduced cross-sections for ^{208}Pb for the $3s_{1/2}$ orbit with perpendicular kinematics. The kinematics are $E_i = 412$ MeV and the proton kinetic energy $T_p = 100$ MeV. The solid line is the full DWBA result, the dashed line is the approximate DWBA using the new phase shifts parameterization, and the dotted line is the approximate DWBA with the κ^2-dependent phases.

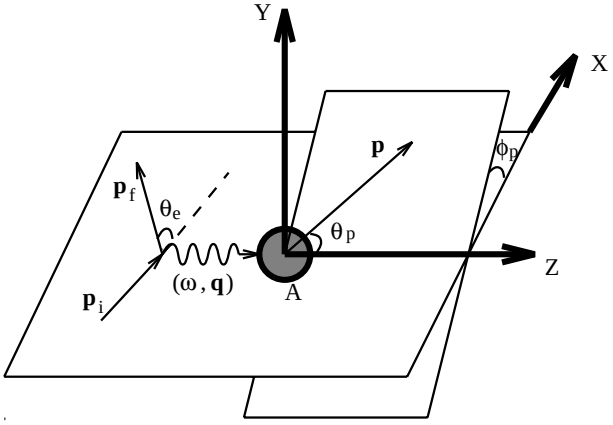

Fig. 3. The coordinate system for the $(e, e'p)$ process.

$(e, e'p)$ reactions with incoming polarized electron beam can be written as

$$\frac{\mathrm{d}^3\sigma}{\mathrm{d}E_f \mathrm{d}\Omega_f \mathrm{d}\Omega_p} = K[v_L R_L + v_T R_T + v_{TT}\cos 2\phi_p R_{TT} + v_{LT}\cos\phi_p R_{LT} + h v_{LT'}\sin\phi_p R_{LT'}] , \quad (6)$$

where $q_\mu^2 = \omega^2 - q^2$ is the four-momentum transfer, and R_L, R_T, R_{TT}, R_{LT}, and $R_{LT'}$ are the longitudinal, transverse, transverse-transverse, longitudinal-transverse, and polarized longitudinal-transverse structure functions, *i.e.*, the so-called first, second, third, fourth, and fifth structure functions, respectively. ϕ_p is the azimuthal angle of the outgoing proton measured with respect to the electron scattering plane, and h is the helicity of the initial electron. The electron kinematics factor is given by $K = \frac{pE\sigma_{\mathrm{M}}}{(2\pi)^3}$, with σ_{M} the Mott cross-section, and the functions v_L, v_T, etc, depend only on the electron kinematics and are given by

$$v_L = \frac{q_\mu^4}{q^4}, \quad v_T = \tan^2\frac{\theta}{2} - \frac{q_\mu^2}{2q^2}, \quad v_{TT} = -\frac{q_\mu^2}{2q^2},$$
$$v_{LT} = -\frac{q_\mu^2}{q^2}\left(\tan^2\frac{\theta}{2} - \frac{q_\mu^2}{q^2}\right)^{1/2}, \quad v_{LT'} = -\frac{q_\mu^2}{q^2}\tan\frac{\theta}{2}, \quad (7)$$

where θ represents the electron scattering angle. The structure functions are defined as

$$\begin{aligned} R_L &= W_{00}\,, \qquad R_T = W_{11} + W_{22}\,, \\ \cos 2\phi_p R_{TT} &= W_{11} - W_{22}\,, \\ \cos\phi_p R_{LT} &= W_{01} - W_{10}\,, \\ \sin\phi_p R_{LT'} &= -i(W_{02} + W_{20})\,, \end{aligned} \quad (8)$$

where the nuclear tensor $W_{\mu\nu}$ is given in terms of a sum over the bound and final spin projections of the proton:

$$W_{\mu\nu} = \sum_{s_i s_f} N_\mu^* N_\nu \,. \quad (9)$$

The quantity N^μ is the Fourier transform of the nucleon current density and is given by

$$N^\mu = \int J^\mu e^{i\mathbf{q}\cdot\mathbf{r}}\, \mathrm{d}^3 r. \quad (10)$$

The nucleon current is given by

$$J^\mu(\mathbf{r}) = e\bar{\psi}_f(\mathbf{r})\left(F_1\gamma^\mu + F_2\frac{i\mu_p}{2M}\sigma^{\mu\nu}q_\nu\right)\psi_b(\mathbf{r})\,, \quad (11)$$

where F_1 and F_2 are the Dirac and the Pauli nucleon form factors and $\mu_p = 1.793$ denotes the proton anomalous magnetic moment. The wave function for the bound state ψ_b is taken from a relativistic Hartree model [25]. The final-state wave function ψ_f is obtained by solving the Dirac equation with an optical potential which comes from the analysis of the elastic proton scattering data [26].

In the full DWBA calculations when the electrons are described by the distorted Coulomb waves, the cross-section is no longer separated and takes on a form different from eq. (6):

$$\frac{\mathrm{d}^3\sigma}{\mathrm{d}E_f \mathrm{d}\Omega_f \mathrm{d}\Omega_p} = \frac{1}{2}\frac{2\pi}{I_{\mathrm{in}}}\rho_e\rho_p\sum|H_i|^2\,, \quad (12)$$

where the summation is over the final-states with an average over the initial states and ρ_e (ρ_p) is the density of states of the electron (proton), given by $\frac{pE}{(2\pi)^3}$. I_{in} denotes the initial flux of electrons given by $\frac{p}{E}$. H_i is the transition matrix element

$$H_i = -4\pi\int j_\mu(\mathbf{r})G(r,r')J^\mu(\mathbf{r}')\mathrm{d}^3 r\mathrm{d}^3 r'\,, \quad (13)$$

where $j_\mu(\mathbf{r}) = e\bar{\psi}_f\gamma^\mu\psi_i$ denotes the electron current. ψ_f and ψ_i are the final and initial electron wave functions distorted by the static Coulomb potential of the target nucleus. $J^\mu(\mathbf{r}')$ is given by eq. (11). The Green's function for the electromagnetic field is denoted by $G(r, r')$.

While a separation as in eq. (6) cannot be allowed in the DWBA calculation, the fourth structure function could be obtained by subtracting the cross-sections at azimuthal angles of the outgoing proton $\phi_p = 0$ and $\phi_p = \pi$ and keeping the other electron and outgoing proton kinematics variables fixed. We call a quantity so determined the *apparent* fourth structure function. The apparent fourth structure function is a function of the missing momentum given by

$$R_{LT} = \frac{\sigma^R - \sigma^L}{2Kv_{LT}} , \tag{14}$$

where L (left) and R (right) indicate the left side at $\phi_p = 0$ and the right side at $\phi_p = \pi$ of the cross-section, respectively. Of course, this fourth structure function can be directly calculated in the PWBA. If the incident electron beam is polarized, helicity h=1, one can obtain the fifth structure function by subtracting the down part ($-\pi < \phi_p < 0$) from the up part ($0 < \phi_p < \pi$) of the cross-section with respect to the scattering plane, while all other kinematics variables are kept the same. The apparent fifth structure function can be written as

$$R_{LT'} = \frac{\sigma^U - \sigma^D}{2Kv_{LT'}\sin\phi_p} , \tag{15}$$

where U and D indicate the "up" and "down" part of the cross-section, respectively. This clearly describes the "up-down" asymmetry of the cross-section with respect to the scattering plane. We also calculate another left-right asymmetry, A_{LT}, defined as

$$A_{LT} = \frac{\sigma^R - \sigma^L}{\sigma^R + \sigma^L} . \tag{16}$$

In this case, the kinematics is the same as for the fourth structure function in eq. (14).

On the other hand, by adding the left side and the right side of the cross-section, one can obtain the second structure function as

$$\frac{\sigma^R + \sigma^L}{2Kv_T} = R_T + x(\theta)\left(R_L + \frac{v_{TT}}{v_L}R_{TT}\right) , \tag{17}$$

where $x(\theta) = \frac{v_L}{v_T}$ is a function of the electron scattering angle θ. In this procedure, it is possible to perform several experiments by changing only the incident electron energy and keeping the four-momentum transfer and proton kinematics variables fixed. Equation (17) is a linear function of the variable $x(\theta)$ like the Rosenbluth separation. Conventionally from eq. (17), one can obtain the constant term which becomes the second structure function and the slope which is a mixing of the first and third structure function.

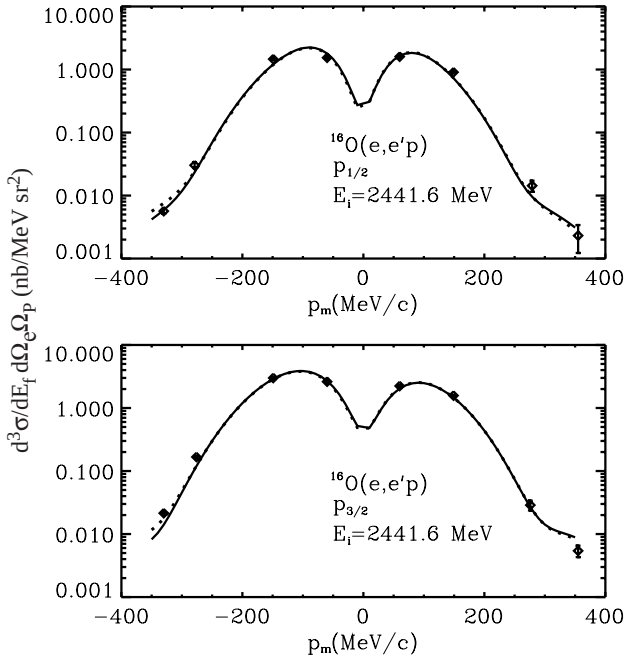

Fig. 4. The cross-sections from the $p_{1/2}$ and $p_{3/2}$ orbits of ^{16}O targets as a function of the missing momentum. The incident electron energy is 2441.6 MeV, the proton kinetic energy is 427 MeV, and the energy transfer is 436 MeV. The solid lines are the approximate DWBA calculations, the dotted lines are the PWBA calculations, and the data are from CEBAF [20].

4 Results

In our analysis we investigate the effect of the Coulomb distortion on the structure functions and the left-right asymmetry with respect to the magnitude of the missing momentum. There are two kinematics in $(e, e'p)$ experiments. One is the parallel kinematics where the outgoing proton momentum $\mathbf{p}$ is along the momentum transfer $\mathbf{q}$. In this case, the three interference structure functions in eq. (6) disappear. The other one is the perpendicular kinematics, the so-called ω-q constant kinematics, where the magnitude of $\mathbf{p}$ is fixed and the polar angle of $\mathbf{p}$ changes with respect to $\mathbf{q}$. We choose only the perpendicular kinematics in order to extract the interference structure functions. Note that all calculations are carried out in the laboratory frame (target fixed frame) and include the proton final-state interaction described by a relativistic optical potential which is obtained from fitting the elastic proton scattering [26]. The outgoing proton is knocked-out from two outer orbits, $p_{1/2}$ and $p_{2/3}$, of the ^{16}O.

In fig. 4, we show the cross-sections as a function of the missing momentum. The electron incoming energy is given by $E_i = 2441.6$ MeV, the ejected proton kinetic energy by $T_p = 427$ MeV, and the energy transfer by $\omega = 436$ MeV. The four-momentum transfer is $Q^2 = q^2 - \omega^2 = 0.8$ (GeV/c)^2. The scattering angle is $\theta = 23.3^\circ$. The solid lines are the approximate DWBA results, the dotted lines are the PWBA results, and the diamonds are data from CEBAF [20]. Note that the full DWBA code cannot evaluate such high electron energy processes, because it needs many angular momentum summations and extensive mod-

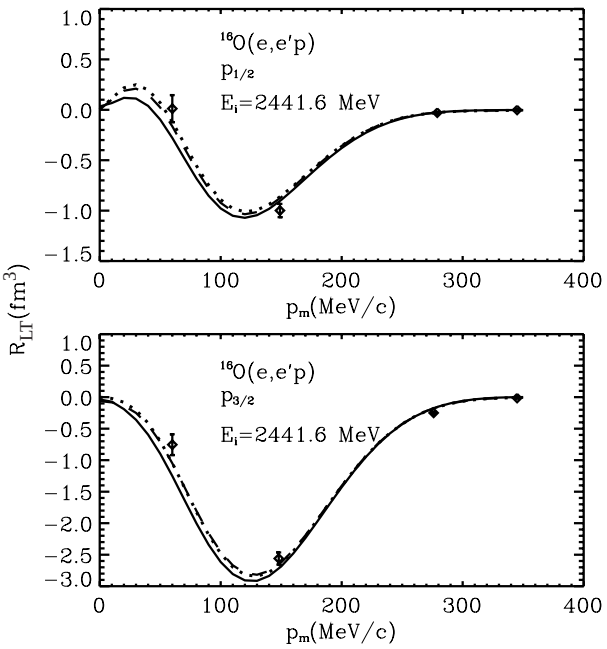

Fig. 5. The fourth structure functions from the $p_{1/2}$ and $p_{3/2}$ orbits of ^{16}O as a function of the missing momentum. The solid lines and the dashed lines are, respectively, the apparent and directly extracted fourth functions for the DWBA results, the dotted lines are the PWBA results, and the diamonds are data from CEBAF [20]. The kinematics is the same as in fig. 4.

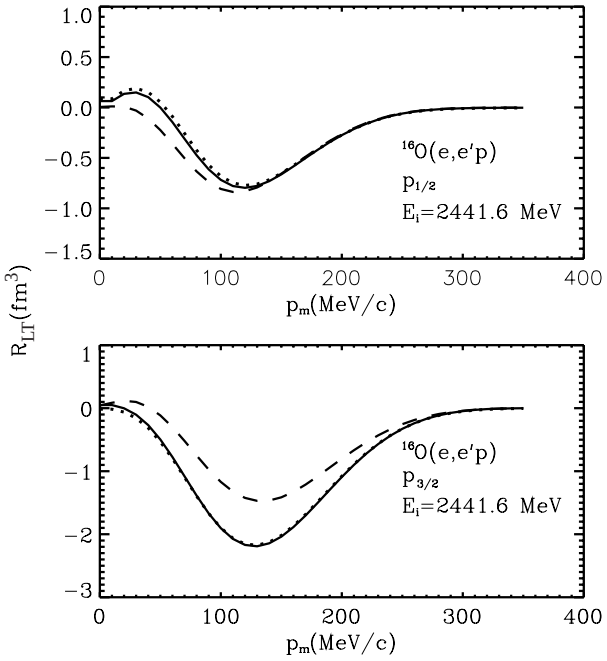

Fig. 6. The fifth structure functions for ^{16}O targets. The azimuthal angle of the knocked-out proton is $\phi_p = 40°$. The solid lines and the dashed lines are, respectively, the apparent and directly extracted fourth functions for DWBA results and the dotted lines are the PWBA calculations.

ifications. Both the PWBA and approximate DWBA results reproduce the experimental data very well. As we expected, the effects of the Coulomb distortion are very small. We perform a linear least χ^2 fit to the data using our relativistic single-particle model for the bound-state wave functions and obtain the spectroscopic factors 0.61 for $p_{1/2}$ and 0.7 for $p_{3/2}$. In the previous work [8] at lower electron energies using the same nuclear model the spectroscopic factors were 0.54 for $p_{1/2}$ and 0.57 for $p_{3/2}$ in comparison with the experimental data from Saclay [28].

In the previous calculations [8,29], the effects of the Coulomb distortion on the cross-sections are of the order of 3%, 7% and 30% for ^{16}O, ^{40}Ca, and, ^{208}Pb, respectively. But, the effects on the fourth structure functions for ^{16}O and ^{40}Ca are about 12–15%, while those on the fourth structure function for ^{208}Pb are higher by a factor of 2 and those on the fifth structure function are about 50% [8,18]. In these calculations, the Coulomb distortion does not affect the shape of the fourth and fifth structure function calculated by the PWBA, although the effect on the magnitude is much greater for these functions than for the corresponding cross-sections.

Figure 5 shows the fourth structure functions with the same kinematics as in fig. 4. The solid lines and the dashed lines are, respectively, the apparent and the directly extracted fourth functions from the approximate DWBA results, the dotted lines are the PWBA results, and the diamonds are the data from CEBAF [20]. In the low missing momentum range ($\leq$ 150 MeV/c), the differences between the solid lines and the dotted lines are of the order of 10% for the $p_{1/2}$ orbit and 5% for the $p_{3/2}$ orbit, while the differences between the dashed lines and the dotted lines are around 2-3% for both orbits. The discrepancy among the solid, the dashed and the dotted lines suggests that the directly calculated fourth structure functions and the apparent fourth structure functions depend on the azimuthal angle of the outgoing proton. Although the separation does not result in a perfect extraction of the structure function, the directly calculated fourth structure functions contain enough physics, *i.e.*, the transition current and the transition density of the target are involved. Of course, for the PWBA calculation the apparent fourth structure function agrees exactly with the directly calculated fourth structure function. Furthermore, although the effects of the electron Coulomb distortion are very small for the cross-section at high incident energy, the effect on the apparent fourth structure functions is a change of about 5-10%. In these calculations, we use the spectroscopic factors extracted from the cross-sections. The shapes generated by the approximate DWBA calculation are the same as these generated by the PWBA calculation in the positions of the minimum and maximum. We also find out that the theoretical calculations for the fourth structure functions and for the cross-sections may need different spectroscopic factors in order to show good agreement with the data. However, the fourth structure functions extracted from the cross-sections may not be well determined due to experimental uncertainties.

In fig. 6, we calculate the fifth structure functions for $p_{1/2}$ and $p_{3/2}$ of ^{16}O at fixed azimuthal angle $\phi_p = 40°$ of the knocked-out proton and with the same electron kinematics as in fig. 4. The solid lines are the apparent and the

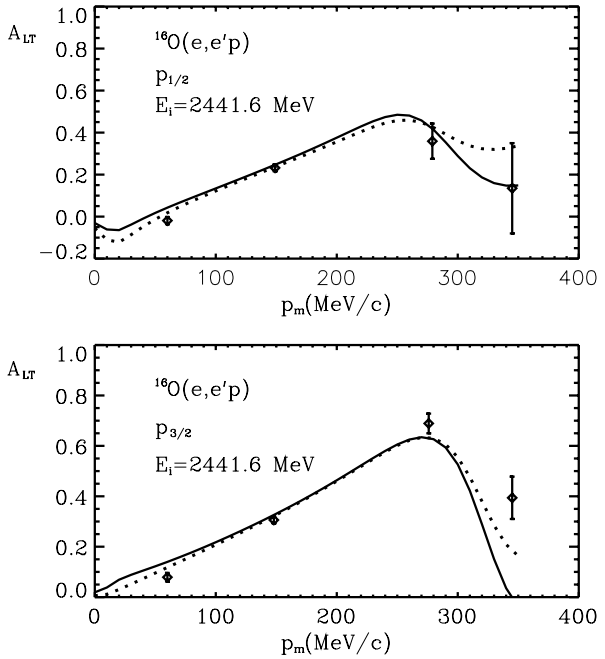

Fig. 7. The asymmetry for the ^{16}O target. The kinematics is the same as in fig. 4.

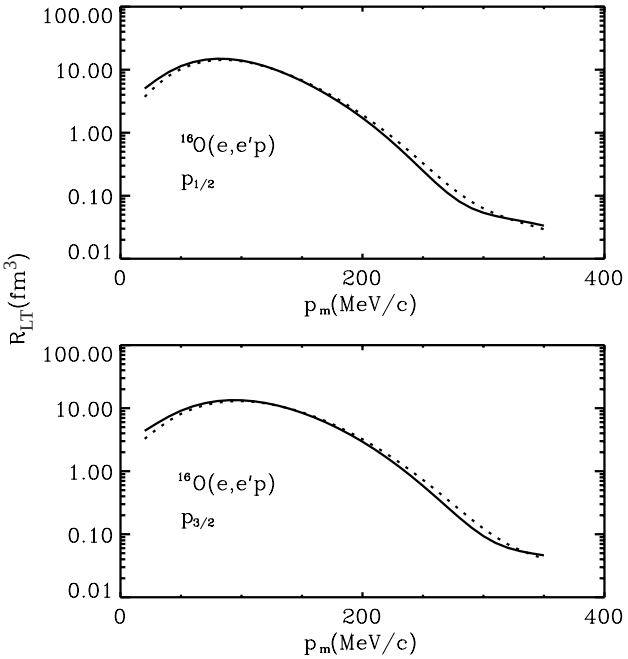

Fig. 8. The second structure functions extracted using the Rosenbluth separation by changing the incident electron energies. The incident electron energies are E_i = 2441.6, 1642.5, and 843.2 MeV. The solid lines are the approximate DWBA calculations and the dotted lines are the PWBA calculations.

dashed lines are the directly extracted fifth functions for the approximate DWBA results and the dotted lines are for the PWBA results. As for the fourth structure functions, the differences between the PWBA and the directly calculated fifth structure functions are around 2-3%, but those for the apparent fifth structure functions appear to be higher by a factor of 2 at the low missing momentum ($\leq$ 150 MeV/c). However, the electron Coulomb distortion does affect the magnitude of the amplitude of the fifth structure functions, but not their shape as we found for the fourth structure function. Notice also that we used the same spectroscopic factors as in fig. 4.

As shown in fig. 7, we also investigate another asymmetry, the so-called left-right asymmetry given in eq. (16). The kinematics is the same as in fig. 4. Particularly, since this quantity does not require any spectroscopic factor, it is possible to compare the theoretical result with the experimental data. From these theoretical calculations we show that our model for a bound state, the σ-ω model, describes the experimental data reasonably well when the missing momentum is less than 300 MeV/c. The electron Coulomb distortion does not change the basic shape of the left-right asymmetry, although the amplitudes are changed by small amount at low missing momentum (less than 100 MeV/c). These asymmetry functions clearly show a Coulomb effect of about 10% at low missing momentum.

In fig. 8 and fig. 9, we show the second structure functions R_T and $R_L + \frac{v_{TT}}{v_L} R_{TT}$ functions in terms of the missing momentum by applying the Rosenbluth separation method with three incident electron energies. The incident electron energies are E_i = 2441.6, 1642.5, and 843.2 MeV and the corresponding scattering angles are θ = 23.3°, 37.2°, and 100.7°, respectively. Here, we use

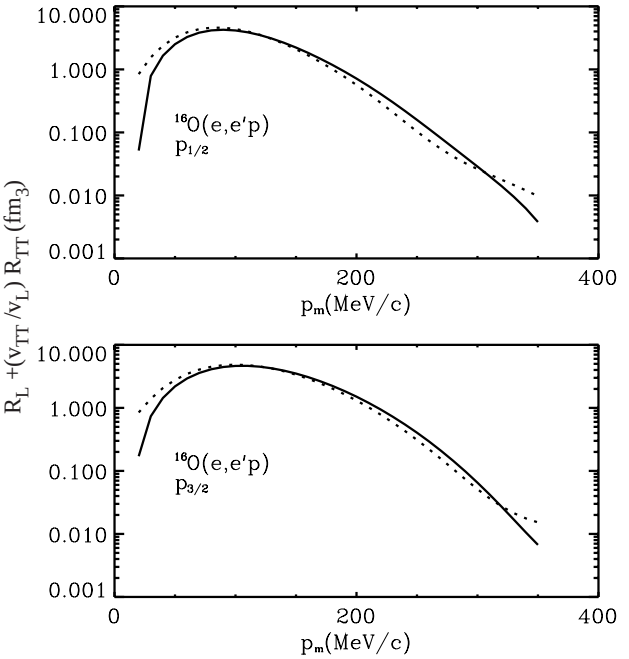

Fig. 9. The $R_L + \frac{v_{TT}}{v_L} R_{TT}$ functions by using the same parameters as in fig. 8.

the same values as in fig. 4 for the knocked-out proton kinetic energy, T_p = 427 MeV, and for the energy transfer, ω = 436 MeV. The four-momentum transfers are also fixed as Q^2 = 0.8 (GeV/c)^2. The peaks for these structure functions lie on the same positions as for the cross-sections. The electron Coulomb effects on the peaks are very small as for the cross-sections but slowly increase on

the side parts. The effects on the second structure function appear smaller than those on the $R_L + \frac{v_{TT}}{v_L} R_{TT}$ function. This clearly shows that the Coulomb effects on the longitudinal term are larger than those on the transverse term because the charge mainly contributes to the longitudinal function. In this case, one cannot compare the apparent and the directly calculated second structure function because of the different incident electron energies used.

5 Conclusion

We have improved our previous approximate method of including Coulomb distortion effects in $(e, e'p)$ reactions from nuclei. The improvement involves a better parameterization of the elastic scattering phase shifts which have the correct behaviour for large angular momenta and require the calculation of only two exact phase shifts (for $\kappa = 1$, and for κ equal to $\mathrm{Int}(pR) + 5$). We show that for the $(e, e'p)$ reaction on ^{208}Pb the cross-section calculated with our approximation using the improved parameterization of the phase shifts agrees quite well with the full DWBA result even beyond the second maximum. This is a significant improvement over the previous approximation for the phase shifts.

In addition, we compare our relativistic single-particle model for the $(e, e'p)$ reaction from ^{16}O with the recently measured cross-section at CEBAF with respect to the $p_{3/2}$ and $p_{1/2}$ shells and investigate the effects of the electron Coulomb distortion on the cross-sections, the second, the fourth, the fifth structure functions, and the left-right asymmetry. The approximate DWBA and PWBA calculations describe the experimental data for the cross-sections very well and the Coulomb effects are very small. We obtain values of the spectroscopic factors equal to 0.61 for $p_{1/2}$ and to 0.7 for $p_{3/2}$. The effects of the electron Coulomb distortion on the structure functions considerably affect the magnitude, while the basic shape and the positions of the maximum and minimum are not changed. We show that it is possible to directly calculate the fourth and fifth structure functions in the presence of the electron Coulomb distortion, although the directly calculated structure functions do not agree exactly with the apparent structure functions. In particular, the fifth structure function describes the final-state interaction, and the left-right asymmetry does not require the spectroscopic factor. By means of the Rosenbluth separation method, it is found that the Coulomb effects on the transverse part are smaller than those on the longitudinal part.

Our improved approximate method of including Coulomb distortion in electron scattering reactions works for high-energy electrons as well as for more moderate energies (300-500 MeV), and for experiments at a few percent level this approximate way of including Coulomb distortion is adequate. The "plane-wave–like" approximation permits the extraction of "structure functions" even in the presence of strong Coulomb effects and thus provides a very good tool for looking into the response of the target nucleus. We suggest that the experiment might be performed for heavy nuclei but with a change of kinematics (from perpendicular to parallel). In particular, if the experiment is performed with parallel kinematics, one can investigate the contribution of the longitudinal term (charge part) by applying the Rosenbluth separation method, so that one can know the effects of the Coulomb distortion, more in detail.

This work was supported by the Korea Research Foundation Grant (KRF-2000-015-DP0086).

References

1. L.I. Schiff, Phys. Rev. **103**, 443 (1956).
2. D.R. Yennie, D.G. Ravenhall, R.N. Wilson, Phys. Rev. **92**, 231 (1953); **95**, 500 (1954).
3. H. Davies, H.A. Bethe, L.C. Maximon, Phys. Rev. **93**, 788 (1954); L.E. Wright, K.K. Sud, D.W. Kosik, Phys. Rev. C **36**, 562 (1987).
4. F. Scheck, M. Stingl, Z. Phys. **209**, 93 (1968).
5. S.T. Tuan, L.E. Wright, D.S. Onley, Nucl. Instrum. Methods **60**, 70 (1968).
6. Yanhe Jin, D.S. Onley, L.E. Wright, Phys. Rev. C **45**, 1311 (1992).
7. Yanhe Jin, D.S. Onley, L.E. Wright, Phys. Rev. C **45**, 1333 (1992).
8. Yanhe Jin, D.S. Onley, L.E. Wright, Phys. Rev. C **50**, 168 (1994).
9. J.M. Udias, P. Sarriguren, E. Moya de Guerra, E. Garrido, J.A. Caballero, Phys. Rev. C **48**, 2731 (1993).
10. C.F. Williamson, T.C. Yates, W.M. Schmitt, M. Osborn, M. Deady, P.D. Zimmerman, C.C. Blatchley, K.K. Seth, M. Sarmiento, B. Parker, Yahne Jin, L.E. Wright, D.S. Onley, Phys. Rev. C **56**, 3152 (1997).
11. Yanhe Jin, J.K. Zhang, D.S. Onley, L.E. Wright, Phys. Rev. C **47**, 2024 (1993).
12. J. Knoll, Nucl. Phys. A **201**, 289 (1973); **223**, 462 (1974).
13. F. Lenz, R. Rosenfelder, Nucl. Phys. A **176**, 513 (1971); F. Lenz, thesis, Freiburg (1971).
14. C. Giusti, F.D. Pacati, Nucl. Phys. A **473**, 717 (1987).
15. M. Traini, S. Turck-Chieze, A. Zghiche, Phys. Rev. C **38**, 2799 (1988); M. Traini, Phys. Lett. B **213**, 1 (1988).
16. M. Traini, M. Covi, Nuovo Cimento A **108**, 723 (1995).
17. K.S. Kim, L.E. Wright, Yanhe Jin, D.W. Kosik, Phys. Rev. C **54**, 2515 (1996).
18. K.S. Kim, L.E. Wright, Phys. Rev. C **56**, 302 (1997).
19. K.S. Kim, Myung Ki Cheoun, Il-Tong Cheon, Yeungun Chung, Eur. Phys. J. A **8**, 131 (2000).
20. Juncai Gao, Ph.D dissertation, MIT (1999).
21. K.S. Kim., L.E. Wright, Phys. Rev. C **60**, 067603 (1999).
22. P. Guéye *et al.*, Phys. Rev. C **60**, 044308 (1999).
23. K.S. Kim, L.E. Wright, D.A. Resler, nucl-th 0103032, to be published in Phys. Rev. C (2001).
24. S. Boffi, C. Giusti, F.D. Pacati, Nucl. Phys. A **435**, 697 (1985).
25. C.J. Horowitz, B.D. Serot, Nucl. Phys. A **368**, 503 (1981).
26. S. Hama, B.C. Clark, E.D. Cooper, H.S. Sherif, R.L. Mercer, Phys. Rev. C **41**, 2737 (1990).
27. T. de Forest Jr., Nucl. Phys. A **392**, 232 (1983).
28. L. Chinitz *et al.*, Phys. Rev. Lett. **67**, 568 (1991).
29. S. Frullani, J. Mougey, Adv. Nucl. Phys. **14**, 1 (1984).